Materials Science-Poland, 40(3), 2022, pp. 80-92
http://www.materialsscience.pwr.wroc.pl/
DOI: 10.2478/msp-2022-0034

Influence of air plasma spraying process parameters on the thermal barrier coating deposited with micro- and nanopowders

Tadeusz Kubaszek[1,*], Marek Góral[1], Paweł Pędrak[1]

[1]Research and Development Laboratory for Aerospace Materials, Rzeszow University of Technology, Powstancow Warszawy 12, 35-959 Rzeszow, Poland

This study investigates the optimal conditions to deposit a thermal barrier coating using micro- and nanopowders in the air plasma spraying (APS) process. The influence of the APS process parameters on the thickness, porosity and hardness of the yttria-stabilized zirconia (YSZ; $ZrO_2 \times 8Y_2O_3$) coatings deposited with a single-electrode plasma gun was determined. The temperature and velocity of melted particles were determined by the DPV diagnostic system to decrease the number of experimental processes. The current and H_2 flow rate were changed in this research. Metco-6700 YSZ micropowder has already been used in plasma spray physical vapor deposition. The results of this study suggest the possibility of using it for APS. The particles of this powder are characterized by high temperature (2,700°C–2,900°C) and high speed (>380 m/s). The highest thickness of the coating was obtained with 6 NLPM (normal liter per minute) H_2 flow and 800 A current. Difficulties were observed with the feeding of the powder particles at higher H_2 flow. The results showed that using APS, deposition of Metco-6609, a nanopowder normally used in suspension plasma spraying, is possible. In this research, this powder was fed using a carrier gas. The coatings were around 40 μm thick and had high porosity. The lowest porosity of the coating was obtained at a current of 600 A and H_2 flow rate of 12 NLPM. In the coatings, unmelted spherical particles were also visible.

Keywords: *thermal barrier coatings, air plasma spraying, yttria-stabilized zirconia, nanopowders*

1. Introduction

The development of modern aeroengines is associated with superalloys that can withstand high temperatures approaching 1,150°C. The turbines in these engines operate at much higher temperatures due to the cooling air distributed within advanced monocrystalline airfoils and the use of thermal barrier coatings (TBCs) [1]. The aim of achieving the highest possible rotor inlet temperature is to increase the thermal efficiency of the engine for economic reasons. However, despite the development of new aeroengine designs, their efficiency is still below the ideal efficiency determined by the combustion of the fuel under stoichiometric conditions, mainly because of the need to increase cooling air flow. Therefore, new materials and coatings for high-pressure turbines are required for further progress [2].

Multilayer TBCs are still the most effective way to reduce the substrate temperature of the hot components of aircraft engines. At the same time, they have led to an increase in rotor inlet temperature and have directly improved the performance of aeroengine turbines [3]. TBCs are characterized by a multilayer structure: a metallic bond coat (multicomponent NiCoCrAlY alloy or diffusion aluminide layer) and an outer ceramic layer (usually yttria-stabilized zirconia [YSZ; $ZrO_2 \times 8Y_2O_3$]) are produced on a Ni superalloy substrate [4]. The metallic bond coat increases the protection of the substrate material against oxidation and ensures proper adhesion of the ceramic layer. The resistance of the bond coat to high-temperature oxidation depends on a layer of thermally grown oxides (TGO) – mainly Al_2O_3 – formed between the ceramic layer and the metallic bond coat during turbine operation. The ceramic layer lowers the temperature at the TBC cross section due to its low thermal conductivity. This layer is directly exposed

* E-mail: tkubaszek@prz.edu.pl

© Kubaszek et al. 2022. This is an open access article distributed under the Creative Commons Attribution-NonCommercial-NoDerivatives 4.0 License. (http://creativecommons.org/licenses/by-nc-nd/4.0/)

to varying thermal and mechanical stresses, including environments of hot oxidation gases [5].

Currently, in the aerospace industry, the outer ceramic layer of the TBC is most commonly produced by the following processes: air plasma spraying (APS) and electron beam physical vapor deposition (EB-PVD) [6]. APS is commonly used to produce a protective ceramic layer in applications, such as combustion chamber components or stationary blades as well as wear-resistant coatings [7]. The ceramic layer produced by the APS process is characterized by a lamellar structure, a porosity of 4%–15%, and many microcracks. This structure provides good heat transfer insulation to the bond coat and substrate material due to the thermal conductivity coefficient equaling 0.83 W/(m·K). However, it is not very resistant to changes in thermal and mechanical stresses [5]. Ceramic layers with greater durability under these conditions are deposited using the EB-PVD process [8]. The high cost of the EB-PVD process, however, limits its application only to the critical components of aeroengines, the rotating blades of the first and second stages of a high-pressure turbine. This is because of the requirement of low surface roughness and high resistance to thermal and mechanical loads. The ceramic coatings produced by this process are characterized by a columnar structure, which provides an increase in resistance to cracking with a low thermal conductivity coefficient of 1.71 W/(m·K) [5].

Currently, the development of deposition processes for protective coatings includes plasma spray physical vapor deposition (PS-PVD) [9] and suspension plasma spraying (SPS) [10]. Literature data [9, 11–13] and the results of our own research [14, 15] indicate that in both processes, viz., PS-PVD and SPS, it is possible to deposit a ceramic coating with good thermal and physical properties using YSZ powder with small particle sizes ($<$10 μm). It is also possible to control its porosity [16, 17] and obtain thermal conductivity values similar to coatings obtained with APS [18, 19]. Several studies [11, 20] have also found that the coatings obtained with PS-PVD and SPS are characterized by higher erosion resistance and resistance to high-temperature oxidation and thermal fatigue compared to the layers in the EB-PVD process, which are characterized by particularly high costs. However, the use of powders with small particle sizes ($<$10 μm) in the SPS and PS-PVD processes is associated with higher implementation costs compared to the conventional APS process. The SPS process requires the use of a suspension feeder and changes in the design of the nozzle that feeds the suspension into the plasma stream [12]. On the other hand, to carry out the PS-PVD process, it is necessary to achieve low pressure in the working chamber (about 1.50 mbar) and to use a high-powered plasma torch $>$150 kW [21].

Research [22, 23] is on to develop process conditions for the spraying of ceramic coatings using powders with micro- and nanometric particle sizes $<$20 μm in the APS process. Dwivedi et al. [22] determined the effect of the size of the YSZ powder particles on the fracture resistance of the film coatings. They found that fracture toughness depended on the porosity of the coating and that the introduction of powder with smaller particle sizes (10–45 μm) resulted in coatings with lower porosity and twice the fracture toughness compared to coatings produced with powder particles of larger diameters (79–117 μm). Huang et al. [23], in their fractographic studies of the YSZ coating, considered different lamellar interface morphologies. Coatings were produced from powder with particle sizes in the range of 15–25 μm and 45–60 μm. The influence of lamellar interface roughness on coating fracture resistance under thermal fatigue and erosion conditions was investigated. They found that the introduction of powders with smaller particle sizes leads to a lower lamellar interface roughness and that the roughness of the lamellar interface also affects crack initiation and crack propagation speed in the coating. Coatings made from coarse-grained powders were shown to have a higher lamellar interface roughness. Compared to coatings made from small particle size powders, these coatings were found to have higher resistance to thermal fatigue and erosion.

A few studies [24, 25] have explored APS processes using micrometric ($<$10 μm) and nanometric ($<$1 μm) particles introduced into the plasma stream through a carrier gas rather than in suspen-

sion, enabling the deposition of ceramic coatings with good properties and replacing PS-PVD and SPS processes, which are more expensive.

2. Experimental details

2.1. Materials

Inconel 625 Ni superalloy with the following chemical composition (wt%) was chosen as the base material: Al: 0.4; C: 0.1; Cr: 22; Co: 1; Fe: 5; Mn: 0.5; Mo: 9; Nb: 3.75; P: 0.015; Si: 0.5; S: 0.015; Ti: 0.4; Ni: balance. This material is characterized by good tensile strength (R_m = 900 MPa) and good heat resistance; therefore, Inconel 625 offers an optimal combination of corrosion resistance and creep, which enable its application in many industries, especially aeronautical technology [26]. In the research, flat samples with dimensions of 25 × 50 × 1 mm were used.

The TBC bond coat was made of a multicomponent NiCoCrAlY alloy plasma sprayed in the APS process on the Inconel 625 superalloy substrate. To deposit the bond coat, Amdry 386 powder (Oerlikon Metco, Wohlen, Switzerland) with the following chemical composition (wt%) was used: Co: 21.5; Cr: 16.3; Al: 14.8; Y: 0.1; Hf: 0.2; Ni: balance.

The outer ceramic layer of the TBC was also produced by APS using three types of Oerlikon Metco YSZ oxide powders. Metco-6609 powder with the smallest particle size D_{10} = 0.1 μm, D_{50} = 0.3–1 μm, and D_{90} = 0.8–2 μm has so far been used mixed with ethanol in suspension in the SPS process [27, 28]. In this investigation, it was fed with a carrier gas in the form of a powder during the APS process. Metco-6700 powder with a particle size of D_{10} = 2 μm, D_{50} = 8 μm, and D_{90} = 18 μm is developed for the deposition of the outer ceramic layer of the TBC with columnar structure in the PS-PVD process [29]. To perform a comparative analysis of the ceramic coatings deposited from micro- and nanopowders, a standard Metco-204NS powder with large particle sizes (D_{10} = 20–28 μm, D_{50} = 49–59 μm, and D_{90} = 90–109 μm) was also examined [30].

2.2. Research methodology

The APS process was carried out using the thermal spraying equipment in the Research and Development Laboratory for Aerospace Materials at the Rzeszow University of Technology, Rzeszów, Poland. An A60 single-electrode torch (Thermico, Dortmund, Germany) with radial powder injection into the plasma plume was used. The powder was fed with a Thermico CPF2 feeder (Thermico, Dortmund, Germany). It allows gravimetric control of the flow rate of the powder independently of the grain size.

The data [31] and the results of previous research [25] clearly show that the properties of the deposited ceramic layer in the TBC are most influenced by the current and the chemical composition and flow rate of the plasma gas mixture, especially H_2. Therefore, these parameters were changed in the research.

Characterization of the temperature and velocity of the particles moving in the plasma stream was done using the DPV eVolution (Tecnar, Saint-Bruno-de-Montarville, Canada). Measurements were made at a distance of 100 mm from the plasma torch nozzle (the spraying distance used in the experimental processes). The DPV system enables the displacement of the measuring point in the x- and y-axes, perpendicular to the axis of the torch nozzle, within the range of ±50 mm. Thus, it is possible to measure the temperature and velocity of particles in the zone of the plasma plume with the highest flow rate. The distribution of temperature and particle velocity values on the cross section of the plasma plume with dimensions of 20 × 20 mm for 5 × 5 measurement points, at 4-mm intervals, was also determined. For each point, measurements were made of a fixed number of particles moving in the plasma stream (n=400) or for a duration of 7 s, whichever occurs earlier.

The characterization of the powder particles moving in the plasma plume using a DPV system was the basis for determining the range of conditions for ceramic layer deposition in the APS process using powders of different grain sizes, as provided in Table 1.

Microscopic examination of the fabricated TBC

Table 1. APS process parameters for deposition of YSZ ceramic outer layer of TBC

Process parameters	**Value**
Plasma torch	A60
Plasma gases Ar/H_2 [NLPM]	54/6; 48/12; 42/18
Current [A]	600; 700; 800
Substrate radial velocity [rev/min]	150
Plasma torch feed rate [mm/s]	3
Time of spraying [s]	1,110
Spray distance [mm]	100
Spray angle [°]	90
Carrier gas [NLPM]	6
Powder feed rate [g/min]	10
Angle of powder injection to plasma plume [°]	90

APS, air plasma spraying; NLPM, normal liter per minute; TBC, thermal barrier coating; YSZ, yttria-stabilized zirconia

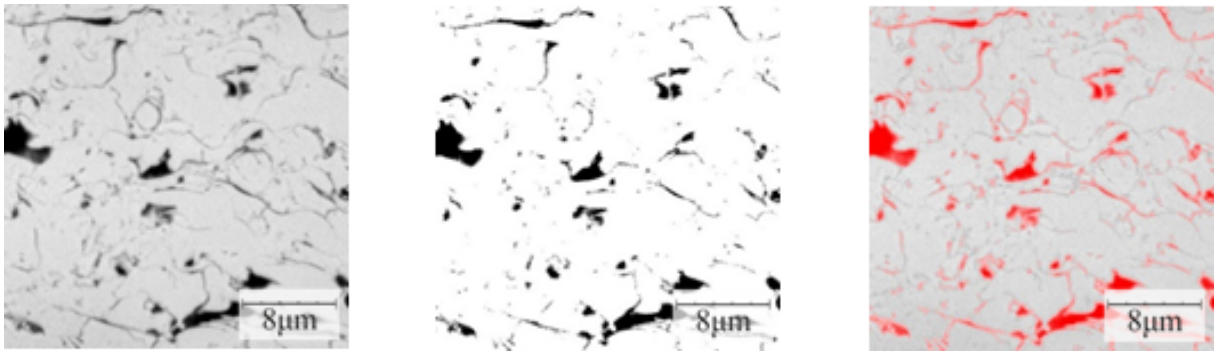


Fig. 1. Microstructure of the TBC YSZ layer: **(A)** initial image; **(B)** after binarization; and **(C)** image after binarization combined with the initial image.
TBC, thermal barrier coating; YSZ, yttria-stabilized zirconia

was performed using a Phenom XL scanning electron microscope (SEM) (Thermo Fisher Scientific, Waltham, MA USA) to determine the thickness and porosity of the outer ceramic layer. An electron beam acceleration voltage of 15 kV and a backscattered electron (BSE) mode were used. The samples were cleaned in isopropyl alcohol solution using an ultrasonic cleaner.

The porosity of the ceramic layer was determined by digital image analysis. For a single layer, 15 images were taken at a magnification of 9,000× with a size of 1,024 × 1,024 pixels. The layered microstructure was binarized using Nikon NIS-Elements (Nikon Instruments Inc., Melville, NY, USA) image analysis software, as presented in Figure 1.

The hardness measurement was carried out using the Vickers method with the Innovatest Nexus 4303 (Innovatest, Maastricht, Netherlands) microhardness tester. A measured force load of 200 gf and a spraying time of 10 s were selected to measure the coatings of various thicknesses. For each plasma-spraying condition, five measurements were taken for the deposited coating.

3. Results and discussion

3.1. Temperature and velocity of molten particles

Measurements of the average temperature and velocity of the $ZrO_2 \times 8Y_2O_3$ oxide powders moving in the plasma stream were carried out using the DPV measuring equipment. It enables one to es-

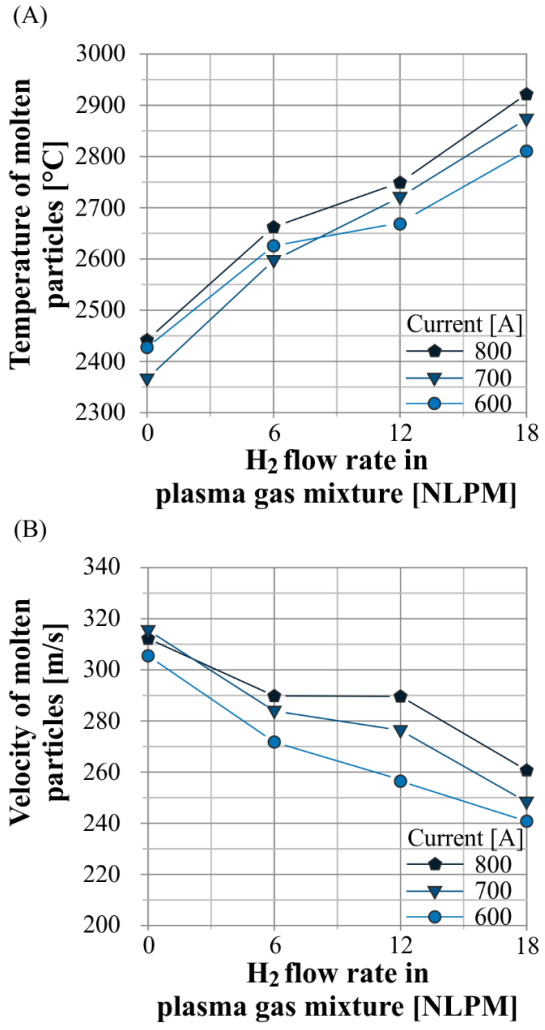


Fig. 2. Dependence of temperature **(A)** and velocity **(B)** of Metco-204NS powder particles in the plasma stream on the H_2 flow rate and the current. NLPM, normal liter per minute

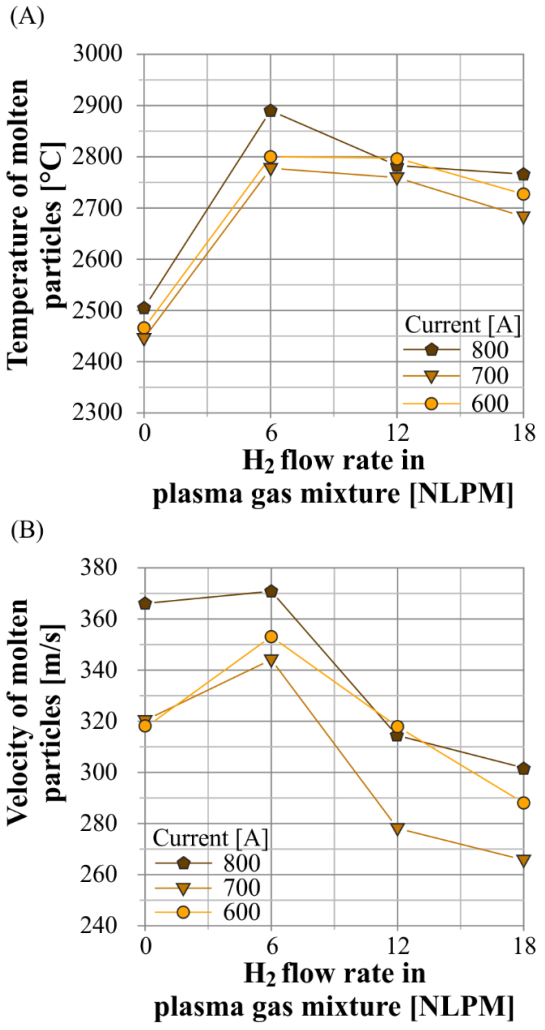


Fig. 3. Dependence of temperature **(A)** and velocity **(B)** of Metco-6700 powder particles in the plasma stream on the H_2 flow rate and the current

tablish how the conditions of the APS process influence the properties of the molten particles and, as a result, the deposited coating. As shown in Figure 2, the mean values of the average temperature and velocity of the melted particles have a linear dependence on the flow rate of H_2 for their radial feed of the Metco-204NS powder into the plasma stream.

Increased plasma energy at a flow rate of $H_2 > 6$ NLPM (normal liter per minute) was found to cause the melting of powder particles. The measurement results also show that as the flow rate of H_2 increases, the mean particle velocity decreases because a higher energy of the plasma stream enables the melting of particles with larger sizes that are characterized by lower velocity. However, the lack of H_2 in the plasma gas mixture leads to a lower temperature. Thus, it is impossible to deposit the ceramic layer with good properties. As a result, it is possible to exclude these processes in experimental APS processes.

The results show that the average temperature of the Metco-6700 powder particles that radially feed into the plasma stream in the A60 plasma torch depends more on the current than the flow rate of

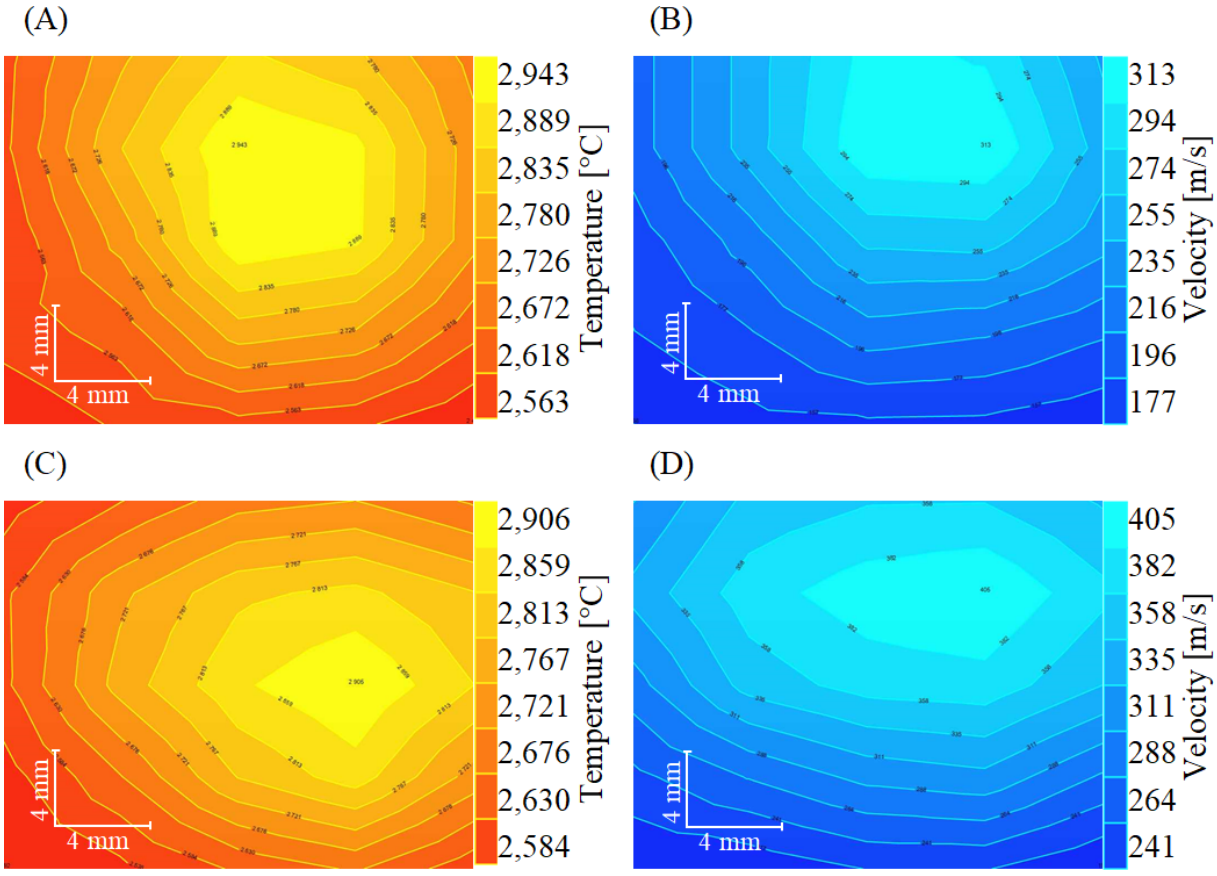


Fig. 4. Contour plot of temperature and velocity of standard Metco-204NS particle **(A, B)** and Metco-6700 micropowder **(C, D)** with APS process parameters: current 800 A; H_2 flow rate 18 NLPM **(A, B)** and 6 NLPM **(C, D)**

H_2, as shown in Figure 3A. Increasing the flow rate of H_2 has little or no effect on the temperature of the melted particles. This effect can occur due to the small difference in the mean particle diameter of the Metco-6700 powder and sufficient plasma stream energy to melt them at the plasma gas flow rate of $H_2 \geq 6$ NLPM. Higher H_2 flow rates could cause difficulties with the radial feed method of highly dispersed powder particles injected into the plasma plume zone with the highest temperature, due to increased plasma enthalpy [32]. In Figure 3B, a linear dependence of the melting particle velocity on the H_2 flow rate was also found in the range of 6–18 NLPM. What is noticeable here is that both the highest temperature (approximately 2,900°C) and the highest particle displacement velocity (370 m/s) were obtained for the H_2 flow rate of 6 NLPM and the current intensity of 800 A. Similarly for Metco-204NS powder measurement, the lack of H_2 in the plasma gas mixture resulted in temperature values that were too low to deposit a ceramic coating with good physical and functional properties. Consequently, for the Metco-6700 powder, these processes were excluded in the experimental tests.

In Figure 4, the comparison of example DPV measurement results can be seen for standard ceramic powder Metco-204NS and micropowder Metco-6700 with H_2 flow rate accordingly of 18 NLPM and 6 NLPM and the current intensity of 800 A (for both powders), which results in the highest-obtained temperature. The temperature was the highest (>2,900°C) in the center of the plasma plume, which proves that Metco-6700 powder particles are transported and melted in the center of the plasma plume despite their average size

(approximately D_{50} = 10–12 μm). The results also show that for Metco-6700 ceramic powder, the velocity was almost 100 m/s higher than for the standard powder, indicating a possible lower density of the deposited coatings.

In the investigation, an attempt was also made to measure the melted powder particles with the smallest diameter D_{50} <1 μm (Metco-6609) using the radial feed method of injecting particles into the plasma stream in the A60 plasma torch. It was found that the particle diameter is below the detection threshold of the DPV eVolution measuring system. Therefore, it is not possible to measure the temperature and velocity of these powder particles. Thus, powders must have a particle size >4 μm.

3.2. Thickness and porosity of ceramic coatings

The main objective of this research was to establish the influence of APS process parameters on the thickness and porosity of ceramic coatings. To evaluate the properties of the coatings deposited with micro and nanopowders (Metco-6700 and Metco-6609), a comparison with the standard Metco-204NS YSZ powder is required.

Figure 5A shows a strong correlation between the thickness of the ceramic coatings deposited with the Metco-204NS powder and the increase in H_2 flow rate. The thickest ceramic coatings (100–120 μm) were obtained only for the flow rate of $H_2 \geq 12$ NLPM and current >700 A. Thermal energy has been shown to be sufficient to melt powder particles with average diameter D_{50} = 49–59 μm. These results are consistent with the DPV measurements shown in Figure 3A. The highest temperature (2,900°C) results in the thickest coating. As seen in Figure 5B, the porosity of the coatings depends more on the current than on the H_2 flow rate. As visible in Figure 5C, the hardness of the obtained coatings slightly increases with the H_2 flow rate from 500 HV0.2 at 6 NLPM to 570 HV0.2 at 18 NLPM, which may be caused by the increase in the thickness of the coating. An exception is for the process with the lowest current (600 A) and H_2 flow rate (6 NLPM) when the coating had only 320 HV0.2, whereby the low temperature and velocity of the particle and the low thickness of the coating result in weak bond strength. The application of high current (800 A) and H_2 flow rates (12 NLPM) simultaneously leads to the lowest porosity (10%) of the deposited coatings. In Figures 6A and 6B, we see that the outer ceramic layer of the TBC produced from the largest particle-diameter powder, Metco-204NS, introduced radially into the plasma plume in the A60 torch, is characterized by a lamellar structure, typical of plasma-sprayed coatings, with visible spherical pores, interlayer porosity, and microcracks resulting from thermal stress relaxation. The surface of the outer layer of the ceramic heat barrier coating exhibits the morphology consisting of (i) areas with well-melted particles and (ii) areas with recrystallized small-diameter particles with a characteristic spherical shape, which is visible in Figure 6C.

Until now, in the aerospace industry, $ZrO_2 \times 8Y_2O_3$ oxide powder with a smaller average particle diameter of D_{50} = 10–12 μm (Metco-6700) has been used mainly in PS-PVD processes [33]. The results show that it is possible to deposit a ceramic coating with the radial powder feed method in the plasma stream (using an A60 single-electrode plasma torch) using a powder with small particles, Metco-6700. As can be seen in Figure 7A, the ceramic coatings with the highest thicknesses of 82 μm and 92 μm were obtained for the process with a current of 700 A and 800 A, respectively, and flow rate of H_2 6 NLPM, which is consistent with the highest temperature and velocity measured on the DPV system for this set of parameters. For the other APS process parameters, the thickness of the deposited coatings was only 50–64 μm. These process parameters also result in the smallest porosity of the coating (<8%), which can be seen in Figure 7B. Furthermore, it was found that the high H_2 flow rate (12 NLPM), regardless of the current (in the examined range: 600–800 A), leads to problems with the radial introduction of the powder with a large particle dispersion, Metco-6700, into the highest temperature zone of the plasma jet. Therefore, the ceramic layers for these process conditions were characterized by a small thickness (50–64 μm) and high porosity (9%–12%). Furthermore, it also

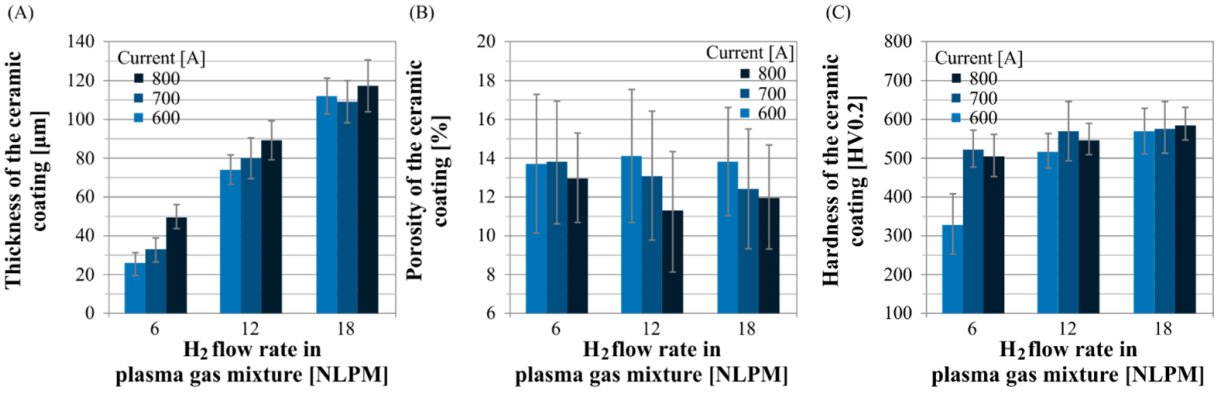


Fig. 5. Dependence of thickness **(A)**, porosity **(B)**, and hardness **(C)** of the TBC ceramic layer on the current and H_2 flow rate, with the use of Metco-204NS ceramic powder.
NLPM, normal liter per minute; TBC, thermal barrier coating

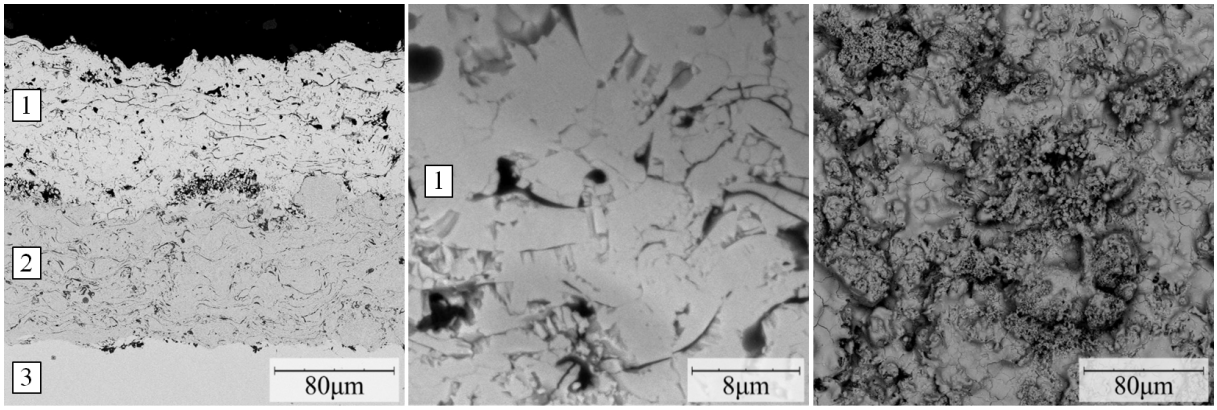


Fig. 6. Microstructure **(A, B)** and surface morphology **(C)** of the TBC ceramic layer deposited from Metco-204NS powder using 800 A current and 12 NLPM flow rate of H_2. 1: YSZ ceramic layer; 2: NiCoCrAlY metallic bond coat; and 3: Inconel 625 substrate material.
NLPM, normal liter per minute; TBC, thermal barrier coating; YSZ, yttria-stabilized zirconia

affects the hardness of the ceramic coatings, which is shown in Figure 7C. The thickest coating with the smallest porosity obtained at 6 NLPM H_2 flow rate and 800 A results in the highest hardness of the coating (542 HV0.2) – similar to the hardness of the ceramic coatings deposited with the standard Metco-204NS powder, discussed above. Increasing the H_2 flow rate to 12 NLPM caused lower hardness values (400–470 HV0.2), which could be caused by lower coating thickness (50–64 µm). For this reason, the radial feed method should be used for a powder with micrometric particle sizes, such as Metco-6700, with a high current and a low flow rate of H_2 of 6 NLPM. It can be seen in Figures 8A and 8B that the use of the smaller particle-diameter powder, Metco-6700, leads to the formation of a lamellar-structured layer (similar to that of standard powder), but with visibly smaller pore sizes and a noticeably larger number of pores in the areas of the interlayer boundaries formed by the YSZ powder particles. The use of Metco-6700 in the APS process also increases the area with visible recrystallized particles compared to areas with well-melted particles, which is evident in the surface morphology shown in Figure 8C.

The Metco-6609 YSZ ceramic powder is gener-

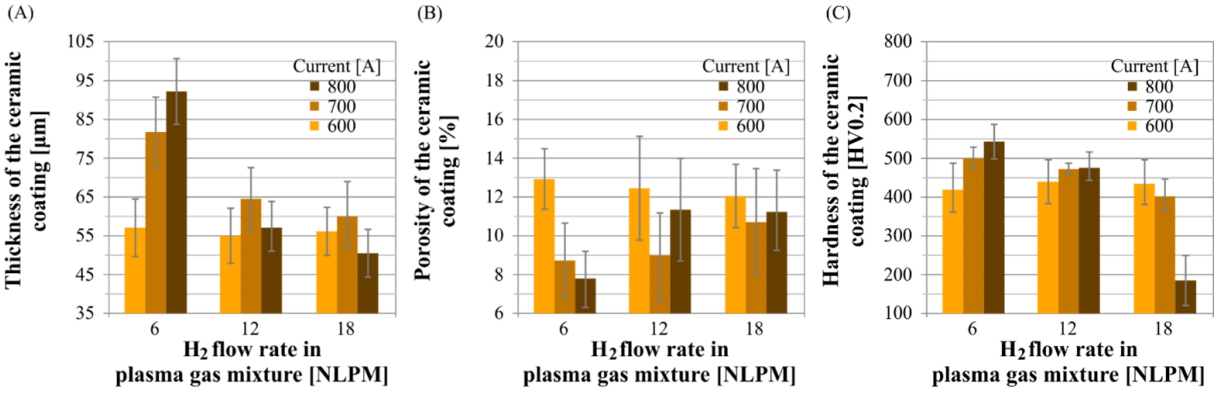


Fig. 7. Dependence of thickness **(A)**, porosity **(B)**, and hardness **(C)** of the TBC ceramic layer on the current and H_2 flow rate, with use of Metco-6700 ceramic powder.
NLPM, normal liter per minute; TBC, thermal barrier coating

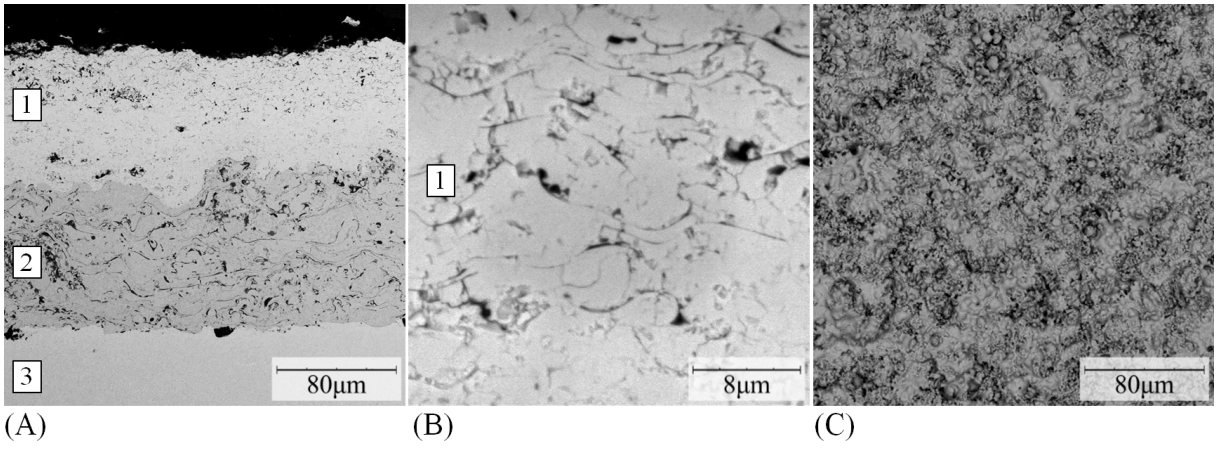


Fig. 8. Microstructure **(A, B)** and surface morphology **(C)** of the TBC ceramic layer deposited from Metco-6700 powder using 800 A current and 6 NLPM flow rate of H_2. 1 – YSZ ceramic layer; 2 – NiCoCrAlY metallic bond coat; 3: Inconel 625 substrate material.
NLPM, normal liter per minute; TBC, thermal barrier coating; YSZ, yttria-stabilized zirconia

ally used mixed with ethanol in suspension plasma spray [27]. In the present research, this powder was fed into a plasma plume using a carrier gas. Due to the fact that the particle diameter is below the detection threshold of the DPV eVolution measuring system, the influence of APS process parameters on thickness and porosity was studied only by metallographic examination.

The layers produced were <40 µm thick irrespective of the process parameters, as shown in Figure 9A. This phenomenon is likely caused by the large dispersion of Metco-6609 powder particles (D_{50} <1 µm) and their low weight, which renders them difficult to be feed into the plasma plume zone with the highest temperature. Figure 9B shows that the deposited layers are also characterized by high porosity (16%–40%). One possible explanation for such high porosity is that a large number of small particles of this powder melt and evaporate in a short time in the plasma stream and recrystallize before reaching the surface of the substrate, or the particles are moving in the outer zone of the plasma plume where there is a lower temperature; the particles in this zone of the plasma are not heated to the melting point of the $ZrO_2 \times 8Y_2O_3$ oxide. Either

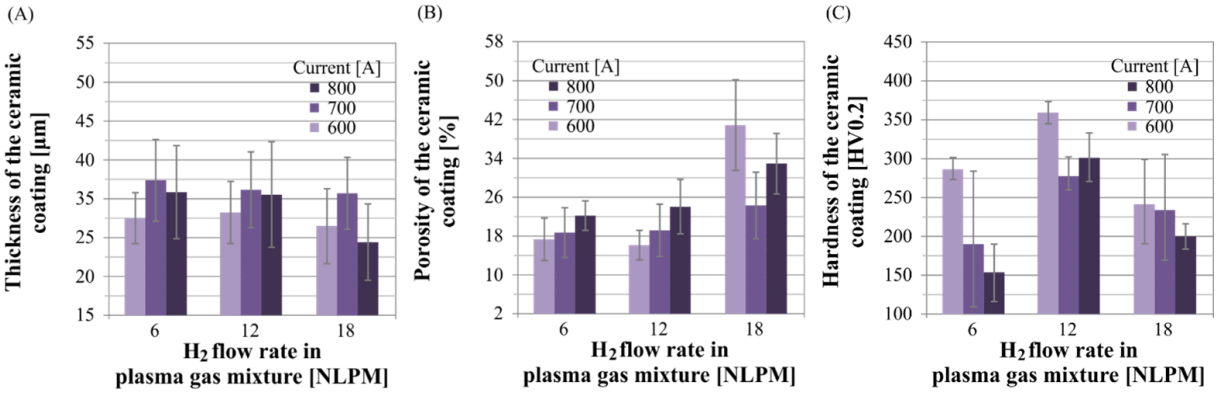


Fig. 9. Dependence of thickness **(A)**, porosity **(B)**, and hardness **(C)** of the TBC ceramic layer on the current and H_2 flow rate, with use of Metco-6609 ceramic powder.
NLPM, normal liter per minute; TBC, thermal barrier coating

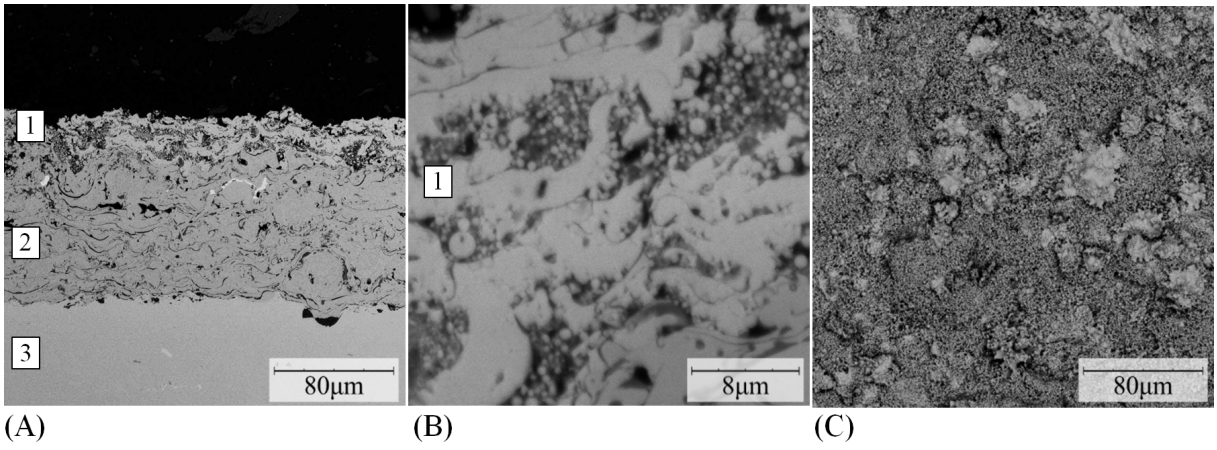


Fig. 10. Microstructure **(A, B)** and surface morphology **(C)** of the TBC ceramic layer deposited from Metco-6609 powder using 600 A current and 12 NLPM flow rate of H_2. 1 – YSZ ceramic layer; 2 – NiCoCrAlY metallic bond coat; 3 – Inconel 625 substrate material.
NLPM, normal liter per minute; TBC, thermal barrier coating; ; YSZ, yttria-stabilized zirconia

way, small spherical particles are visible in the microstructure in Figures 10A and 10B. Similar effects have been observed in the PS-PVD process [34]. The large spray distance in this process leads to the recrystallization of the oxide vapors of $ZrO_2 \times 8Y_2O_3$ before they reach the surface of the substrate. The deposited ceramic layer of the TBC is then characterized by a quasi-columnar structure: between the columnar grains, there are recrystallized spherical $ZrO_2 \times 8Y_2O_3$ oxide particles. Hence, the deposited coating is characterized by low hardness (<300 HV0.2), as shown in Figure 9C. Due to the differences in porosity between coatings caused by different volumes of well-melted particles and small spherical particles (e.g., visible in Figure 10B), the value of hardness is in the range of 150–300 HV0.2. Therefore, the deposition of nanosized ceramic powder using a carrier gas and the radial feed method leads to a microstructure that is not very promising, compared to the YSZ columnar structure coating produced by SPS using Metco-6608 (a suspension version of Metco-6609 powder) [27, 35].

The lowest porosity and the highest hardness of the examined APS process parameters examined were found in the ceramic layer deposit with 12

NLPM H_2 flow and 600 A current, making them the most suitable values when using radial powder fed into the plasma plume. As with Metco-6700 powder, the use of nanometric Metco-6609 powder fed radially into the plasma plume increases the proportion in surface morphology with visible recrystallized particles compared to well-melted areas, as seen in Figure 10C.

In summary, results show that the use of the same ceramic material (YSZ) causes a different lamellar structure depending on the size of the powder particles. The Metco-6700 micrometric powder resulted in a less-porous coating with significantly smaller pore sizes and a higher number in the interlayer boundaries compared to coatings deposited with standard Metco-204NS powder with the same thickness (approximately 100 μm) and only for processes with a low H_2 flow rate $\leq$ 6 NLMP. The coatings obtained by such a process were characterized by a similar hardness >500 HV0.2. The use of Metco-6609 nanometric powder resulted in a coating with spherical particles and remelted areas; therefore, the porosity of these coatings was higher than that of the other powders used in the study. The coatings were characterized by hardness about twice smaller than that of the Metco-204 and Metco-6700 coatings. Such a result indicates that this powder is not suitable for spraying in the APS process with its radial feed method. In further research, the axial introduction of this powder in the Axial III multielectrode torch will be studied, where problems with introducing a powder particle into the plasma plume can be avoided, and the properties of the coatings, e.g., resistance to oxidation, thermal properties, and bond nature of the coatings, can be tested.

4. Conclusions

Based on the results obtained from the conducted research and their analysis, it can be concluded that it is possible to produce ceramic coatings using $ZrO_2 \times 8Y_2O_3$ oxide powders with micrometric (<10 μm) and nanometric (<1 μm) particle sizes, using the APS process. The following conclusions were established:

1. The determination of the thermal and physical properties, viz., temperature and velocity of the YSZ particles moving in the plasma jet, enables one to reduce the number of experimental technological processes necessary to determine the correct plasma spraying process conditions.
2. The developed plasma spraying process conditions made it possible to establish the influence of torch current (in the range of 600–800 A) and H_2 flow rate (in the range of 6–18 NLMP) on the thickness, porosity, and hardness of the ceramic layer of the TBC.
3. The outer ceramic layer of the TBC produced by plasma spraying of Metco-6700 micropowder and Metco-6609 nanopowder is characterized by a thickness and porosity of approximately 100 μm and <8%, respectively, for Metco-6700 and 40 μm and 16%, respectively, for Metco-6609 when optimal APS process conditions are used.
4. The hardness of the ceramic coatings deposited by Metco-6700 micropodwer is similar to that of the coatings produced by standard Metco-204NS powder (>500 HV0.2) for coatings with equivalent thickness (approximately 100 μm).
5. The deposited ceramic layers are characterized by a lamellar structure comparable to that obtained with the standard Metco-204NS powder.
6. The average temperature and velocity of the melted particles depend linearly on the H_2 flow rate for the Metco-204NS powder; the thickness of the deposited coating depends more on the H_2 flow rate, while porosity depends more on the current.
7. The highest temperature (approximately 2,900°C) and the highest particle displacement velocity (370 m/s) were obtained for the lowest flow rate of H_2 (6 NLPM) and the highest current (800 A) for the Metco-6700 powder, resulting in the highest thickness of the obtained coating (approximately 100 μm) and the lowest porosity.

References

[1] Dimiduk DM, Perepezko JH. Mo-Si-B alloys: developing a revolutionary turbine-engine material. MRS Bull. 2003;28(9):639–45. https://doi.org/10.1557/mrs2003.191

[2] Perepezko JH. The hotter the engine, the better. Science. 2009;326(5956):1068–9. https://doi.org/10.1126/science.1179327

[3] Darolia R. Thermal barrier coatings technology: critical review, progress update, remaining challenges and prospects. Int Mater Rev. 2013;58(6):315–48. https://doi.org/10.1179/1743280413Y.0000000019

[4] Moskal G, Swadźba L, Mendala B, Góral M, Hetmańczyk M. Degradation of the TBC system during the static oxidation test. J Microsc. 2010;237(3):450–5. https://doi.org/10.1111/j.1365-2818.2009.03290.x

[5] Feuerstein A, Knapp J, Taylor T, Ashary A, Bolcavage A, Hitchman N. Technical and economical aspects of current thermal barrier coating systems for gas turbine engines by thermal spray and EBPVD: A review. J Therm Spray Technol. 2008;17(2):199–213. https://doi.org/10.1007/s11666-007-9148-y

[6] Rezanka S, Mack DE, Mauer G, Sebold D, Guillon O, Vaßen R. Investigation of the resistance of open-column-structured PS-PVD TBCs to erosive and high-temperature corrosive attack. Surf Coat Technol. 2017;324:222–35. https://doi.org/10.1016/J.SURFCOAT.2017.05.003

[7] Rakhadilov BK, Kenesbekov AB, Kowalevski P, Ocheredko IA, Sagdoldina ZB. Development of air-plasma technology for hardening cutting tools by applying wear-resistant coatings. News Natl Acad Sci Repub Kazakhstan, Ser Geol Tech Sci. 2020;3(441):54–62. https://doi.org/10.32014/2020.2518-170X.54

[8] Bernard B, Quet A, Bianchi L, Joulia A, Malié A, Schick V, et al. Thermal insulation properties of YSZ coatings: Suspension Plasma Spraying (SPS) versus Electron Beam Physical Vapor Deposition (EB-PVD) and Atmospheric Plasma Spraying (APS). Surf Coat Technol. 2017;318:122–8. https://doi.org/10.1016/j.surfcoat.2016.06.010

[9] Goral M, Kotowski S, Sieniawski J. The technology of plasma spray physical vapour deposition. High Temp Mater Process. 2013;32(1):33–9. https://doi.org/10.1515/htmp-2012-0051

[10] Zhou D, Guillon O, Vaßen R. Development of YSZ thermal barrier coatings using axial suspension plasma spraying. Coatings. 2017;7(8):120–37. https://doi.org/10.3390/coatings7080120

[11] von Niessen K, Gindrat M. Plasma spray-PVD: a new thermal spray process to deposit out of the vapor phase. J Therm Spray Technol. 2011;20(4):736–43. https://doi.org/10.1007/s11666-011-9654-9

[12] Sokołowski P, Nylen P, Musalek R, Łatka L, Kozerski S, Dietrich D, et al. The microstructural studies of suspension plasma sprayed zirconia coatings with the use of high-energy plasma torches. Surf Coat Technol. 2017;318:250–61. https://doi.org/10.1016/j.surfcoat.2017.03.025

[13] Fauchais P, Vardelle M, Goutier S, Vardelle A. Key challenges and opportunities in suspension and solution plasma spraying. Plasma Chem Plasma Process. 2014;35(3):511–25. https://doi.org/10.1007/s11090-014-9594-5

[14] Góral M, Kubaszek T, Kotowski S, Sieniawski J, Dudek S. Influence of deposition parameters on structure of TBCS deposited by PS-PVD method. Solid State Phenom. 2015;227:369–72. https://doi.org/10.4028/www.scientific.net/SSP.227.369

[15] Góral M, Kubaszek T. The influence of process parameters on structure of ceramic coatings deposited by PS-PVD method. Solid State Phenom. 2017;267:243–7. https://doi.org/10.4028/www.scientific.net/SSP.267.243

[16] Bacciochini A, Ben-Ettouil F, Brousse E, Ilavsky J, Montavon G, Denoirjean A, et al. Quantification of void networks of as-sprayed and annealed nanostructured yttria-stabilized zirconia (YSZ) deposits manufactured by suspension plasma spraying. Surf Coatings Technol. 2010;205(3):683–9. https://doi.org/10.1016/j.surfcoat.2010.06.013

[17] Fauchais P, Etchart-Salas R, Rat V, Coudert JF, Caron N, Wittmann-Ténèze K. Parameters controlling liquid plasma spraying: solutions, sols, or suspensions. J Therm Spray Technol. 2008;17(1):31–59. https://doi.org/10.1007/s11666-007-9152-2

[18] Łatka L, Cattini A, Pawłowski L, Valette S, Pateyron B, Lecompte JP, et al. Thermal diffusivity and conductivity of yttria stabilized zirconia coatings obtained by suspension plasma spraying. Surf Coat Technol. 2012;208:87–91. https://doi.org/10.1016/j.surfcoat.2012.08.014

[19] Bernard B, Schick V, Remy B, Quet A, Bianchi L. High temperature thermal properties of columnar yttria stabilized zirconia thermal barrier coating performed by suspension plasma spraying. J Phys Conf Ser. 2016;745:1–8. https://doi.org/10.1088/1742-6596/745/3/032012

[20] Algenaid W, Ganvir A, Calinas RF, Varghese J, Rajulapati KV, Joshi S. Influence of microstructure on the erosion behaviour of suspension plasma sprayed thermal barrier coatings. Surf Coat Technol. 2019;375:86–99. https://doi.org/10.1016/j.surfcoat.2019.06.075

[21] Hospach A, Mauer G, Vaen R, Stöver D. Columnar-structured thermal barrier coatings (TBCs) by thin film low-pressure plasma spraying (LPPS-TF). J Therm Spray Technol. 2011;20(1–2):116–20. https://doi.org/10.1007/s11666-010-9549-1

[22] Dwivedi G, Viswanathan V, Sampath S, Shyam A, Lara-Curzio E. Fracture toughness of plasma-sprayed thermal barrier ceramics: influence of processing, microstructure, and thermal aging. J Am Ce-

ram Soc. 2014;97(9):2736–44. https://doi.org/10.1111/jace.13021

[23] Huang J, Wang W, Lu X, Liu S, Li C. Influence of lamellar interface morphology on cracking resistance of plasma-sprayed YSZ coatings. Coatings. 2018;8(5):1–15. https://doi.org/10.3390/coatings8050187

[24] Gao Y, Zhao Y, Yang D, Gao J. A novel plasma-sprayed nanostructured coating with agglomerated-unsintered feedstock. J Therm Spray Technol. 2016;25(1–2):291–300. https://doi.org/10.1007/s11666-015-0340-1

[25] Kubaszek T, Góral M. Influence of air plasma spraying process parameters on ceramic layer in thermal barrier coatings. Solid State Phenom. 2017;267:207–11. https://doi.org/10.4028/www.scientific.net/SSP.267.207

[26] Chyrkin A, Gunduz KO, Fedorova I, Sattari M, Visibile A, Halvarsson M, et al. High-temperature oxidation behavior of additively manufactured IN625: Effect of microstructure and grain size. Corros Sci. 2022;205(December 2021):110382. https://doi.org/10.1016/j.corsci.2022.110382

[27] Aranke O, Gupta M, Markocsan N. Microstructural evolution and sintering of suspension plasma-sprayed columnar thermal barrier coatings. J Therm Spray Tech. 2019;28(1–2):198–211. https://doi.org/10.1007/s11666-018-0778-z

[28] Oerlikon Metco. Metco 6609 – material product data sheet Internet.. cited 2022 Nov 14. https://www.oerlikon.com/ecoma/files/DSM-0406.2_ZrO2_8Y2O3_Suspensions.pdf (accessed 2022-11-14)

[29] Mauer G, Vaßen R. Plasma Spray-PVD: plasma characteristics and impact on coating properties. J Phys Conf Ser. 2012;406(1):012005. https://doi.org/10.1088/1742-6596/406/1/012005

[30] Oerlikon Metco. Metco 204NS – material product data sheet Internet.. cited 2022 Nov 14. https://www.oerlikon.com/ecoma/files/DSM-0242.5_8YO_ZrO_HOSP.pdf (accessed 2022-11-14)

[31] Fauchais PL, Heberlein JVR, Boulos MI. Thermal spray fundamentals. Boston: Springer; 2014. https://doi.org/10.1007/978-0-387-68991-3_1

[32] Nicoll AR, Gruner H, Prince R, Wuest G. Thermal spray coatings for high temperature protection. Surf Eng. 1985;1(1):59–71. https://doi.org/10.1179/sur.1985.1.1.59

[33] Liu SH, Trelles JP, Murphy AB, He WT, Shi J, Li S, et al. Low-pressure plasma-induced physical vapor deposition of advanced thermal barrier coatings: microstructures, modelling and mechanisms. Mater Today Phys. 2021;21:100481. https://doi.org/10.1016/j.mtphys.2021.100481

[34] Zhang B, Wei L, Guo H, Xu H. Microstructures and deposition mechanisms of quasi-columnar structured yttria-stabilized zirconia coatings by plasma spray physical vapor deposition. Ceram Int. 2017;43(15):12920–9. https://doi.org/10.1016/j.ceramint.2017.06.190

[35] Seshadri RC, Dwivedi G, Viswanathan V, Sampath S. Characterizing suspension plasma spray coating formation dynamics through curvature measurements. J Therm Spray Technol. 2016;25(8):1666–83. https://doi.org/10.1007/s11666-016-0460-2

Received 2022-10-03
Accepted 2022-12-13